ANNALI DI GEOFISICA, VOL. XXXVII, N. 5, September 1994

Statistical study of epicentre alignment in the broader Aegean area

Patrizia Tosi (1), **Valerio De Rubeis** (1), **Eleftheria Papadimitriou** (2) **and Petros Dimitriu** (2)
(1) *Istituto Nazionale di Geofisica, Roma, Italy*
(2) *Laboratory of Geophysics, Aristotelian University of Thessaloniki, Greece*

Abstract
Accurate data concerning shallow (h ≤ 60 km) earthquakes ($M_s \geq 4.5$) that occurred in the broader Aegean area are used to point out the presence of linear seismogenic structures (seismolineaments). The earthquake data were analyzed by the use of a specific algorithm, and the directions of the best alignment of epicentres were found. The algorithm is based on statistical criteria applied within a circular area with the aim of searching for the best direction of alignment; this is then tested, to discriminate whether or not the pattern could stem from a random distribution of epicentres, or whether it is effectively the result of a linear seismic structure; the procedure is repeated to cover the whole area examined. The resulting lineaments can be regarded as individual tectonic units, as they usually coincide with known active faults or fault systems. An interpretation is given of the spatio-temporal evolution of the seismicity along the lineaments in terms of the asperity model.

Key words *Aegean area – epicentre – seismolineament – faults interaction*

1. Introduction

The Aegean and the surrounding area is considered to be one of the most seismically active regions of the world, since it constitutes one of the most rapidly deforming continental regions. The region is bounded on the north by stable continental blocks of the Eurasian plate, on the west by the Adriatic Sea, on the east by central Turkey, and on the south by oceanic material of the African plate. Since the Miocene, the locus of subduction of the African plate beneath Eurasia, the present Hellenic trench, has been migrating southwards with respect to Eurasia. Briefly, the most prominent features of tectonic origin are, from south to north: the Mediterranean ridge, a compressional submarine accretionary prism of material that extends from the Ionian Sea to Cyprus; the Hellenic trench with a maximum water depth of 5 km; the Hellenic arc, which consists of the outer sedimentary arc and the inner volcanic arc; and finally, the back-arc Aegean area (Papazachos and Comninakis, 1969, 1971).

The basic seismotectonic features of the area (fig. 1) can be summarized as follows (Papazachos *et al.*, 1991): a) thrust faulting along the coasts of Western Greece, Albania and southwestern ex-Yugoslavia as a result of the continental collision between the Adriatic microplate and the Greek mainland; b) thrust faulting along the convex side of the Hellenic arc due to the subduction of the African oceanic lithosphere under the Aegean; c) a strike-slip dextral fault zone in the northwestern end of the Hellenic arc (Ionian Islands); d) normal faults dominating the inner part of the Aegean and the surroundings, except for Northwestern Anatolia and Northern Aegean where strike-slip dextral faults are observed. To explain these two last systems of faults a single model was proposed by Taymaz *et al.* (1991) and discussed in Jackson (1993), in which the systems are the expression of the relative motion of two sets of fault-bounded

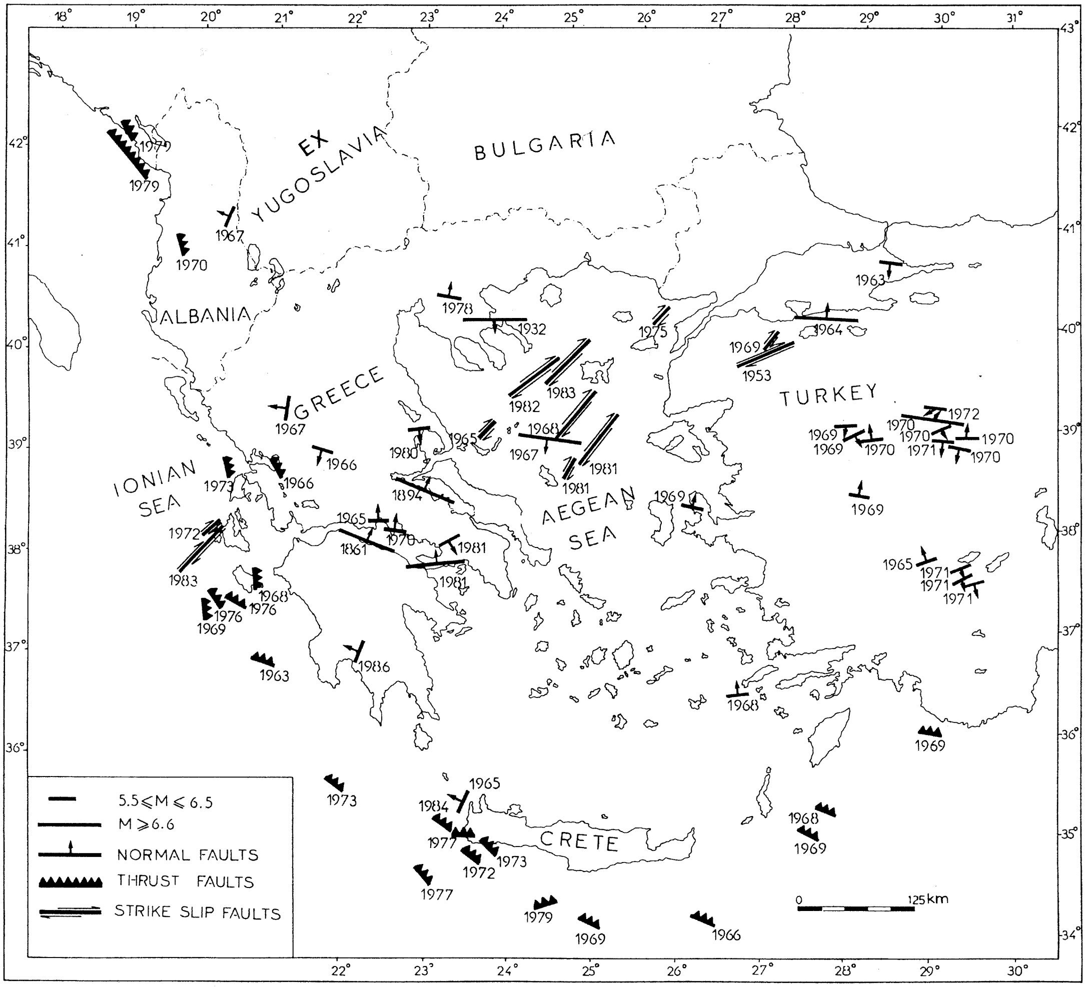

Fig. 1. Schematic representation of the main tectonic features of the Aegean and surrounding area as derived from tectonic data and focal mechanisms of shallow earthquakes; the numbers are the year of occurrence of the corresponding event (from Papazachos *et al.*, 1992).

blocks; in particular the strike-slip system rotates slowly anti-clockwise while the normal system, to west, is characterized by a faster clockwise rotation.

Although the occurrence of strong shallow ($M_s \geq 6.0$) earthquakes in the area is rather frequent (they occurred at a mean rate of one such event per year), detailed mapping of surface fault traces has been performed for a limited number of them. This is because most of these events have their foci in the sea area. To obtain information concerning the orientation of the major active tectonic lines, other indirect methods have been developed and applied. Papazachos *et al.* (1992) used all the available information to determine the orientation of active seismic faults.

In the present paper an attempt is made to apply a statistical method, initially introduced by De Rubeis *et al.* (1991) for the territory of Italy, with the purpose of mapping the most significant and better estimated seismolineaments, indicating the seismogenic structure, by the use of accurate and complete data concerning shallow earthquakes. The obtained results are discussed in the framework of the regional stress pattern.

2. Method of analysis

A specific algorithm has been devised to identify seismic structures and statistically discriminate them from a random distribution of points. In particular, two hypotheses have been verified to recognize an alignment of epicentres. First, a statistically significant distribution of seismic events along a line; and second, a relatively homogeneous distribution of the epicentres on the selected line, to avoid the trivial case of an alignment constituted in reality by events concentrated around one or two points.

In the present analysis all epicentres inside several circles of radius R have been considered and the two conditions mentioned above have been tested, trying as alignments the diameters of each circle with different directions.

The first condition is verified by calculating the quantity

$$V = \frac{\sum_{i=1}^{n} \left(\frac{D_i}{R}\right)^2 M_i}{\sum_{i=1}^{n} M_i} \tag{2.1}$$

where n is the number of epicentres considered, D_i is the Euclidean distance between the i^{th} event and the examined line of alignment, M_i is the magnitude of that event and R is the chosen radius of the circle in which the epicentres lie (fig. 2). It can be seen that V decreases as the events approach the line considered; V can be thought of as the dispersion of the epicentres localizations around the tested line.

In order to statistically discriminate the alignments from a random distribution of points, it is essential to fix a threshold for the V value. To this end a random redistribution of epicentres was conducted, calculating several times the V values. It should be noted that such an operation changed only the coordinates of the events, leaving unaltered their magnitude; this was done to ensure a representation of seismicity as close to reality as possible from the energetic viewpoint, considering that magnitude plays an important weighting role in calculating V. The resulting V population was then ordered in function of the number of events within each circle: for each class of equal number of events a distribution of V values has been obtained; a limit $V_{\lim}$ was then fixed in order to separate the 99% of the elements for each V distribution, the hypothesis being that the remaining values ($V \leq V_{\lim}$) have only 1% probability to stem from a random distribution of epicentres. Figure 3 shows the variation of $V_{\lim}$ for different numbers of random epicentres, obtained with a smoothed cubic spline interpolation of the experimental $V_{\lim}$ data calculated with the random catalogue.

Another factor that affects the choice of valid alignments derives from the errors of localization and magnitude of earthquakes. From the error propagation theory we have

$$\sigma_V = \sqrt{\left(\frac{2}{R^2}\frac{\sum_{i=1}^{n} D_i M_i \sigma_{Li}}{\sum_{i=1}^{n} M_i}\right)^2 + \left(\frac{1}{R^2}\frac{\sum_{i=1}^{n} D_i^2 \sum_{i=1}^{n} M_i - n\sum_{i=1}^{n} D_i^2 M_i}{\left(\sum_{i=1}^{n} M_i\right)^2}\right)^2 \sigma_M^2} \tag{2.2}$$

The first term of the sum is referred to the localization error σ_L, while the second part represents the effect of the magnitude error σ_M; it is easy to see that, essentially, the error on V (σ_V) is small when the radius R is great compared to σ_L (for the other symbols refer to eq. (2.1)).

Taking into account the V value with its related σ_V, a seismic alignment was considered

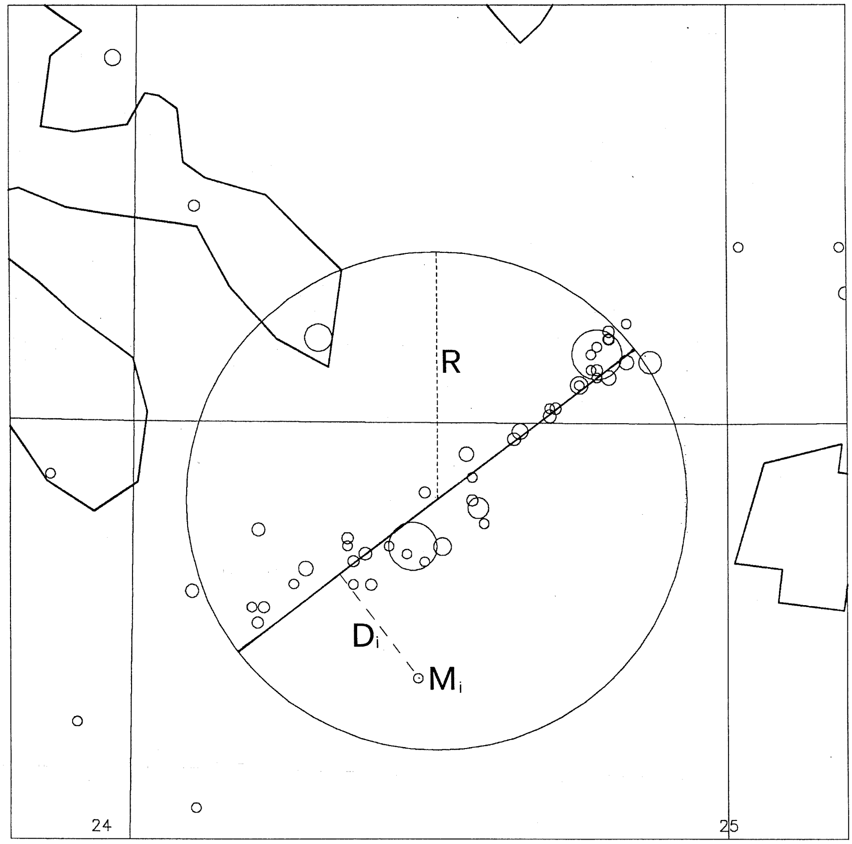

Fig. 2. Example of a circular area in which one test alignment is evidenced: D_i represents the distance of one epicentre to the alignment, as used in expression (2.1): each epicentre has its D_i value which contributes to the calculation of the V value. In each circular area, 18 diameters with different directions are tried, in order to retain the lowest value that will be further statistically checked.

significant if the related V had at least an 84% probability to lie under the respective random threshold (fig. 3).

The second condition, concerning the homogeneity of the points along the selected line, was verified using the χ^2 test. The examined line was divided into 5 equal segments and inside each of them the number n_c of the projections of the epicentres was calculated (weighted by the magnitudes of the events); the obtained frequency distribution was compared to a uniform distribution following the statistical relation:

$$\chi^2 = \frac{\Sigma_{j=1}^{5}(Fo_j - Fu)^2}{Fu} \tag{2.3}$$

where Fo (observed frequency) and Fu (uniform frequency) are defined as:

$$Fo_j = \sum_{k=1}^{n_c} M_k \qquad Fu = \frac{\Sigma_{i=1}^{n} M_i}{5} \tag{2.4}$$

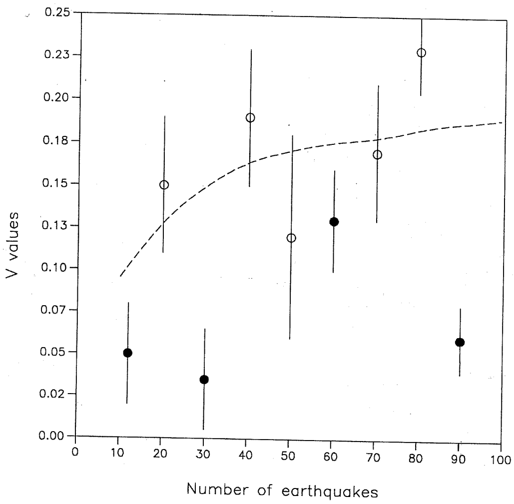

Fig. 3. The dashed line is the smoothed cubic spline interpolation of the limit V values (not shown in figure), stemming from a random distribution of epicentres, in function of the number of events contained in each circular area. Open and filled circles represent some examples of V values calculated on real situations, with their error bars of $\pm 1\sigma_V$; filled circles correspond to significant V values, *i.e.* to be accepted a V value must fall below the dashed limit, the whole length of the error bar included.

The number of classes has been fixed to 5 as a good compromise between a sufficient number of events available inside each class and a high number of classes. Only the alignments satisfying the χ^2 test with a confidence limit better than 1% were retained.

3. Application in the broader Aegean area

The method described above has been applied in the broader Aegean area using a complete and homogeneous catalogue of shallow earthquakes (h $\leq$ 60 km) with magnitudes $M_s \leq 4.5$. The focal parameters of these events which occurred during the time period 1970-1984, were redetermined by Karakostas (1988), with the purpose to achieve an improved accuracy by this determination. The improvement was significant, especially for the focal depths. According to these data, the mean focal depth is about 5 km in the main part of continental Greece and in Western Turkey, 10 km in the Aegean and 20 km along the Hellenic arc.

The total number of earthquake sample is 1739, including 30 earthquakes with magnitude $M_s \geq 6.0$. Figure 4 is a map of the area under study depicting the shallow seismicity of the period 1970-1987. We can see from this map that, except for the larger earthquakes and their associated sequences, the activity is distributed throughout the whole territory.

The analysis was conducted, in more detail, by superposing on the area under investigation a regular grid with a side length of 5 km. Several circles were considered centered on each node, with radii varying from 20 to 60 km (step of 5 km). Inside each circle, eighteen different orientations were tested (varying in all directions with a step of 10 degrees) as possible alignments. In particular, for each direction the values of the two parameters V and χ^2 were calculated as described above using the localizations of the epicentres lying inside the circle; significant lines were retained and drawn together. Figure 5 shows the results obtained by the performed analysis.

Along the coastline of Southern ex-Yugoslavia, Albania and Western Greece the direction of the epicentres delineation (lineaments 1 and 2 in fig. 5) has a NW-SE strike and follows the zone of thrust faulting produced by the convergence taking place in this area. In Cephalonia Island (lineament 3 in fig. 5) the strike-slip faulting trending NE-SW is well defined.

In W. Peloponnese the NW-SE trend of the defined lineament (5 in fig. 5) is in accordance with the faults defined by fault plane solutions and the distribution of the aftershocks of recent strong ($M_s \geq 5.2$) main shocks (Karakostas *et al.*, 1993a,b, 1994).

Along the Hellenic arc, the lineaments (6, 7, 8 and 9, in fig. 5) run parallel to it. The N-S trending structures between Crete and Karpathos Islands (middle portion of lineament 8), as well as between Karpathos and Rodos Islands (lineament 9) are in good agreement with the results of Jongsma and Mascle (1981) who investigated this area by seismic reflection profiling.

In the mainland of Greece, where the predominant stress field is extensional, the direction of the lineaments defined (numbered 10, 11, 12, 13, in fig. 5) is not the same in all the cases. The N-S trend in Albania follows the N-S faulting produced by the E-W extension, taking place along the transitional zone running between the external compressional zone and the N-S extensional zone in the back-arc Aegean area. In Northern Greece, where NE-SW normal faulting is reported (Panagiotopoulos *et al.*, 1993), the defined line 11 is in good agreement with this direction.

In N. Aegean the seismicity is clearly concentrated along the NE-SW trending strike-slip faults (lineaments 18, 19, 20 and 21; fig. 5).

The lineaments so determined can be considered as individual tectonic units, as they coincide, in most of the cases, with known active

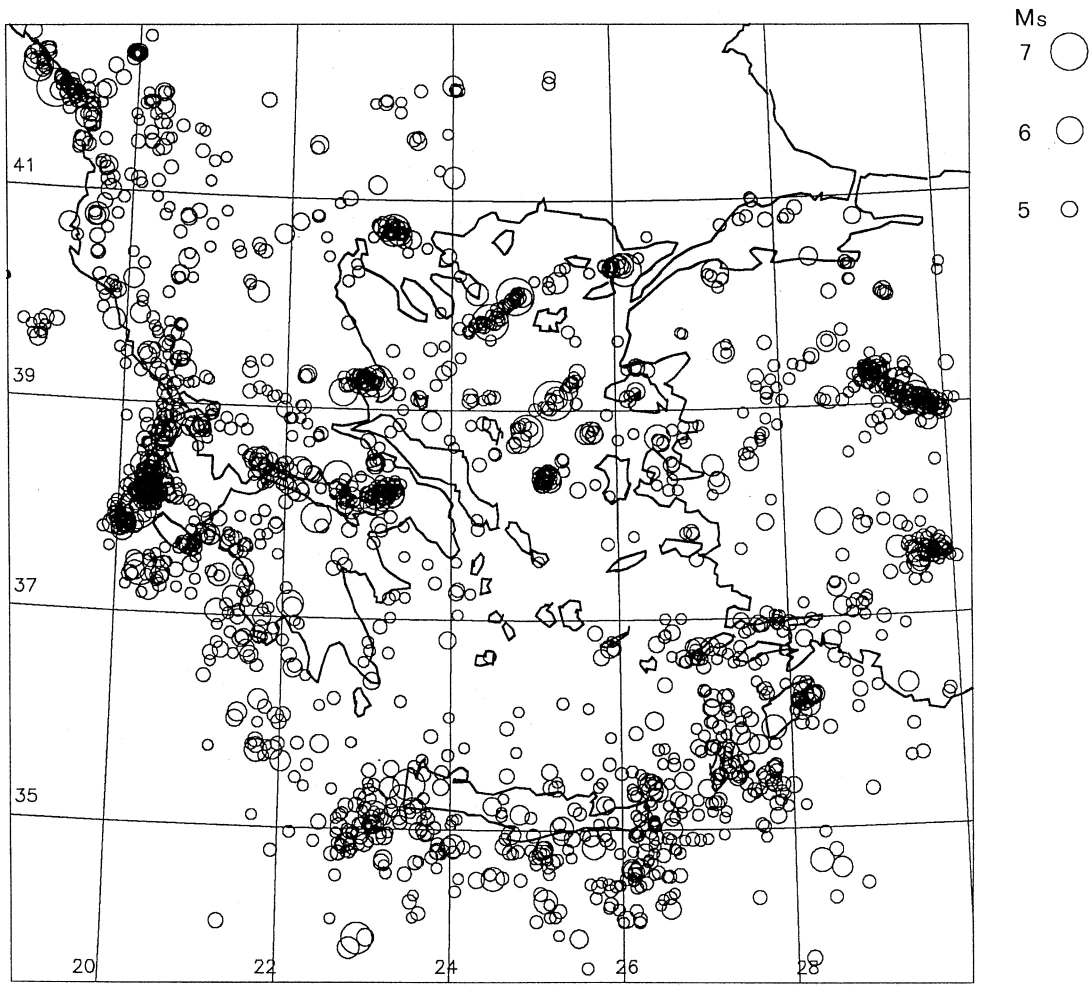

Fig. 4. Shallow seismicity (h ≤ 60 km) in the broader Aegean area during the time period 1970-1984 (data are taken from Karakostas, 1988).

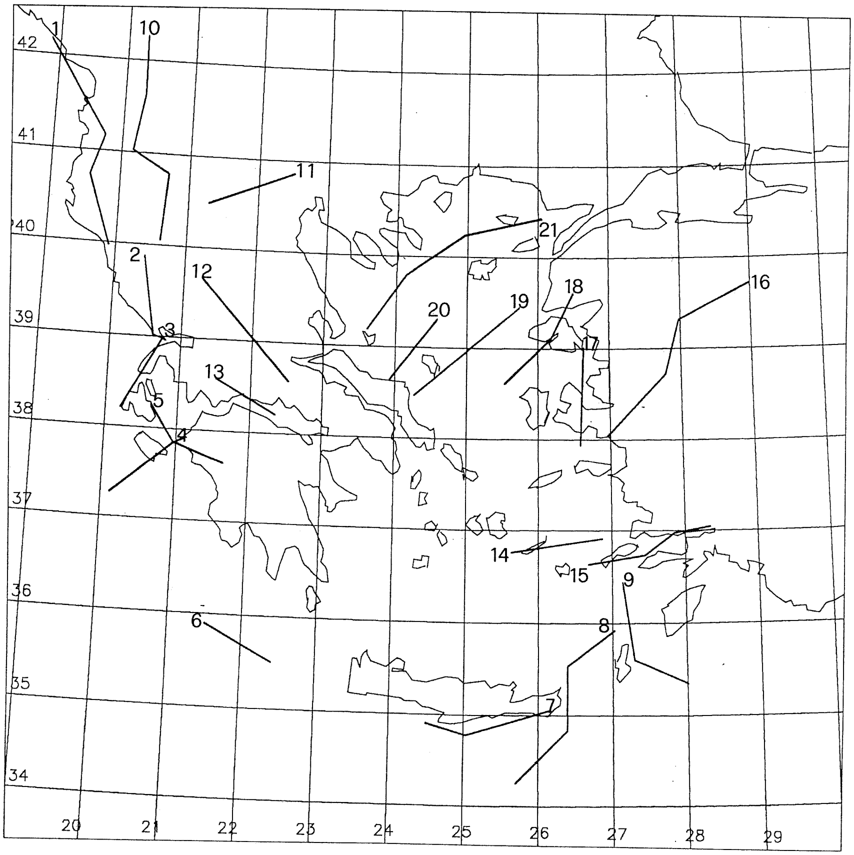

Fig. 5. Seismic alignments determined in the broader Aegean area, by the use of seismicity data for the period 1970-1984.

faults or fault zones. A good agreement is found with the results of Nikolaev and Varushenko (1993) who used microearthquake data for the time period 1978-1989, to construct a map of seismolineaments with eight preselected orientations and then inferred the regional tectonic stress field.

4. Temporal evolution of the seismicity along the lineaments

In order to investigate the time evolution of seismic activity along the found linear structures, several spatio-temporal diagrams have been produced. Some authors used such diagrams as a useful tool to analyze or simply show seismic activity (Matsumura, 1984; Lay and Kanamori, 1981). In the present study a seismic catalogue of the region was used (Comninakis and Papazachos, 1986) starting from the year 1950 and with magnitude larger than 4.5 and the earthquakes with a distance less than 20 km from each alignment were plotted (fig. 6a-d). The vertical axis in each figure represents time and the horizontal axis represents position along the lineament. Each event is characterized by the distance along the

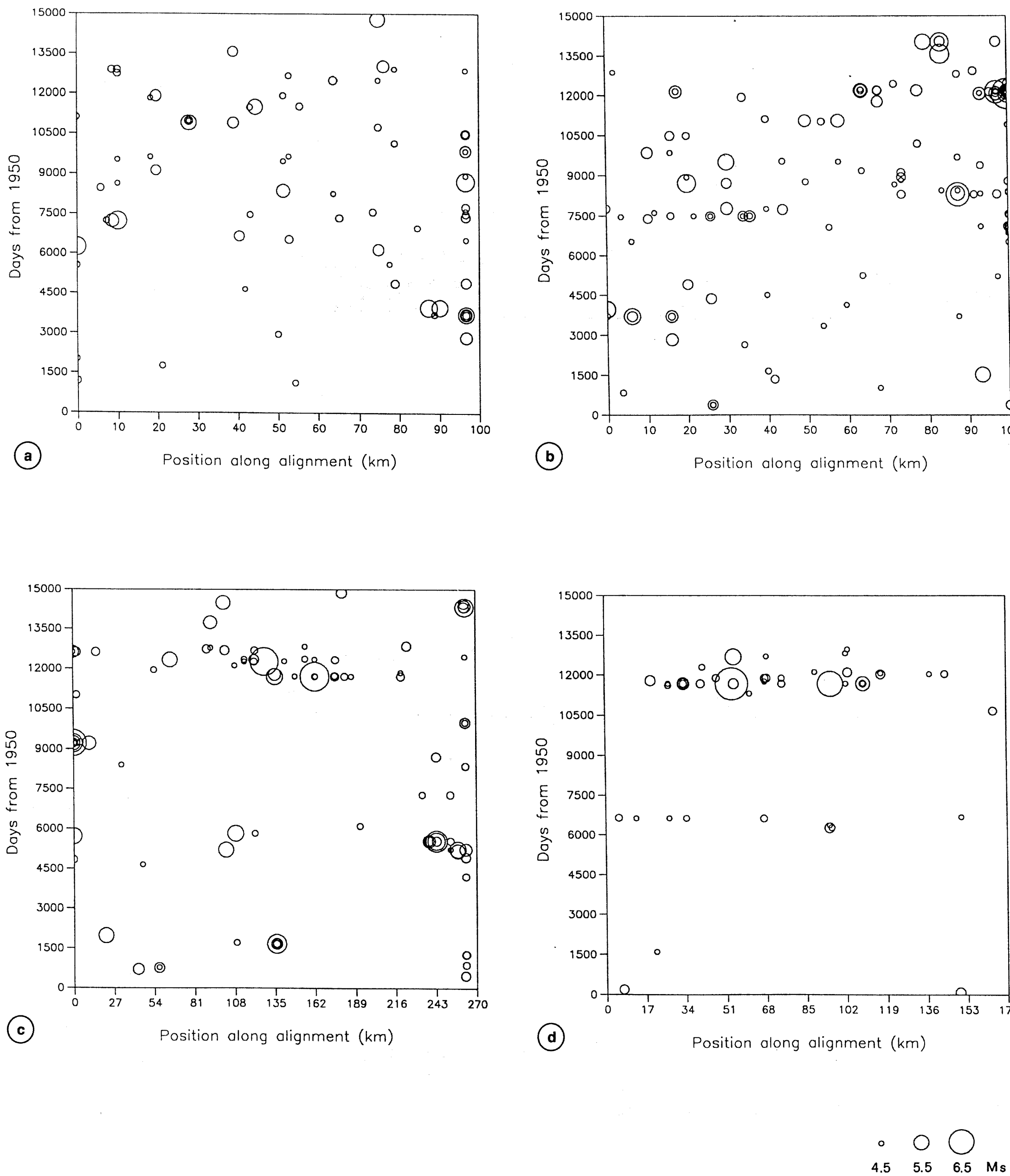

Fig. 6a-d. Space-time plots of the earthquakes related to the alignments 2 (a), 3 (b), 21 (c), 19 (d). The origin position of the alignment (in abscissa) is marked in fig. 5 by the identification number of the structure.

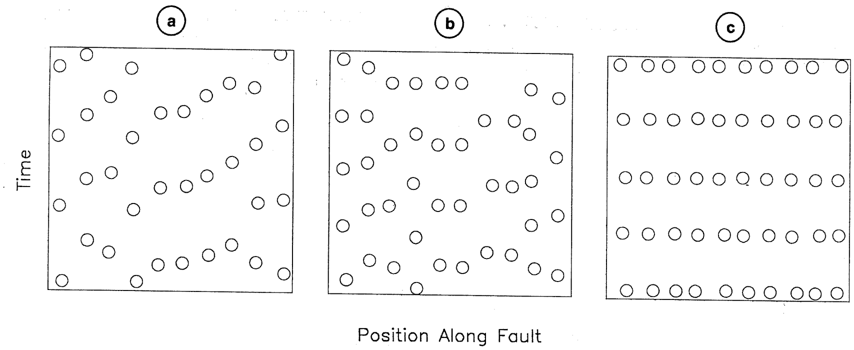

Fig. 7a-c. Earthquake sequences generated with the model of Lay and Kanamori (1981) for variable subfault interaction parameter. a): no subfault interaction; b): moderate subfault interaction; c): strong subfault interaction (redrawn from Lay and Kanamori, 1981).

line measured from one of the edges of the alignment; the time since 1950 is expressed in days.

From the space-time plots of the earthquakes related to each lineament, the behaviour of the seismic activity is examined and interpreted in terms of the asperity model (Lay and Kanamori, 1981). Figure 7a-c shows some representative earthquake sequences generated by this model in which the interaction parameter between subfaults is varied, but the initial random strength distribution is not. In fig. 7a there is no interaction between subfaults. This pattern was produced with only a small range of strengths of the different subfaults, yet clustering of events seldom occurs. Even a small interaction between subfaults produces a markedly greater tendency for sub-zone failures to cluster in time as shown in fig. 7b, though well-separated subfaults show little obvious interaction. Notice that a given length of fault often experiences ruptures spanning only one or two sub-zones, but occasionally a very long rupture occurs. A very strong subfault interaction produces the pattern shown in fig. 7c. There is regular occurrence of great earthquakes rupturing a large portion or the entire length of the fault.

The spatio-temporal diagrams built for the alignments located with our statistical method, can be divided in the three shown categories (a, b, c) with different level of subfault interaction. From this classification comes out that in all the alignments from 1 to 9, that are situated in zones dominated by a compressional stress field, the events are quite independent and clustering rarely occurs (fig. 6a,b); this behaviour is proper of the sequences displayed in fig. 7a,b (type b is more evident in alignments 1, 3 and 5). On the other side, the alignments of the N. Aegean (numbers 18, 19, 20, 21), running parallel to the strike-slip faults, present a marked clustering of the events in time (fig. 6c,d): each alignment shows periods of activity along all the structure, alternated with periods of quiescence. The subfault interaction in this case should be very strong or there is not dishomogeneity segmenting the faults, like the model in fig. 7c.

5. Conclusions

Despite the complexity of the seismotectonic conditions in the broader Aegean area and the resulting complexity of the earthquake spatial distribution, it has been possible to determine certain lineaments along which seismicity seems to gravitate. The method used to assess the alignments is based on statistical tests that guarantee the objectivity of the results. These lineaments can be regarded as individual tectonic units; in fact they usually coincide with known active faults or fault systems. Their direction well agrees with the direction of the known active faults in the studied area, as they were previously defined (Papazachos *et al.*, 1992), in particular along the trust zones (subduction and continental collision) and in the N. Aegean zone of strike-slip faulting.

The analysis of the spatio-temporal evolution of the seismicity along the alignments allows the distinction between homogeneous alignments (with strong interaction between subfaults) and alignments probably constituted by systems of subfaults with poor interaction.

Acknowledgements

The authors would like to express their sincere appreciation to Prof. B.C. Papazachos for the valuable discussions and his suggestions.

REFERENCES

COMNINAKIS, P.E. and B.C. PAPAZACHOS (1986): *A Catalogue of Earthquakes in Greece and the Surrounding Area During the period 1911-1985*, Publ. Geophys. Lab. Univ. Thessal., **1**, 167.

DE RUBEIS, V., C. GASPARINI and P. TOSI (1991): Strutture sismogenetiche in Italia centrale. *Studi Geol. Camerti*, special issue 1991/2, 283-286.

JACKSON, J. (1993): Relations between faulting and continuous deformation on the continents, *Annali di Geofisica*, **36** (2), 3-11.

JONGSMA, D. and J. MASCLE (1981): Evidence for northward thrusting south-west of the Rhodes basin, *Nature*, **293**, 49-51.

KARAKOSTAS, B.G. (1988): Relationship between the seismic activity and geological and geomorphological features of the Aegean and the surrounding area, *Ph. D. Thesis*, pp. 243 (in Greek).

KARAKOSTAS, B.G., E.M. SCORDILIS, CH.A. PAPAIOANNOU, B.C. PAPAZACHOS and D. MOUNTRAKIS (1993a): Focal properties of the October 16, 1988 Killini earthquake (Western Greece), in *Proceedings of the 2nd Congress Hellenic Geophysical Union, Florina, Greece, 5-8 May 1993*, 136-145.

KARAKOSTAS, B.G., G.F. KARAKAISIS, CH.A. PAPAIOANNOU, J. BASKOUTAS, B.C. PAPAZACHOS and J. DRAKOPOULOS (1993b): Preliminary results of the focal properties of the Pyrgos, 1993 earthquake (NW Peloponnese - Greece), in *Proceedings of the 2nd Congress Hellenic Geophysical Union, Florina, Greece, 5-8 May 1993*, 418-426.

KARAKOSTAS, B.G., E.E. PAPADIMITRIOU, D. HATZFELD, D. I. MAKARIS, K.C. MAKROPOULOS, D. DIAGOURTAS, CH.A. PAPAIOANNOU, G.N. STAVRAKAKIS, J. DRAKOPOULOS and B.C. PAPAZACHOS (1994): The aftershock sequence and focal properties of the July 14, 1993 (M_s = 5.4) Patras earthquake, in *Proceedings of the 7th Congress Hellenic Geology Society* (in press).

LAY, T. and H. KANAMORI (1981): An asperity model of large earthquake sequences, in *Earthquake Prediction, an International Review*, edited by D.W. SIMPSON and P.G. RICHARDS, Maurice Ewing ser. vol. 4, (AGU Washington D.C.), 579-592.

MATSUMURA, S. (1984): A one parameter expression of seismicity patterns in space and time, *Bull. Seismol. Soc. Am.*, **74**, 2559-2576.

NIKOLAEV, V.A. and S.S. VARUSHENKO (1993): Reconstruction of the stress field in the area of Greece using seismolineament analysis, in *Proceedings of the 2nd Congress Hellenic Geophysical Union, Florina, Greece, 5-8 May 1993* (abstract).

PANAGIOTOPOULOS, D.G., E.E. PAPADIMITRIOU, CH.A. PAPAIOANNOU, E.M. SCORDILIS and B.C. PAPAZACHOS (1993): Source properties of the 21 December 1990 Goumenissa earthquake in Northern Greece, in *Proceedings of the 2nd Congress Hellenic Geophysical Union, Florina, Greece, 5-8 May 1993*, 286-296.

PAPAZACHOS, B.C. and P.E. COMNINAKIS (1969): Geophysical features of the Greek island arc and Eastern Mediterranean ridge, *C. R. Conference Reunie à Madrid*, **16**, 74-75.

PAPAZACHOS, B.C. and P.E. COMNINAKIS (1971): Geophysical and tectonic features of the Aegean arc, *J. Geophys. Res.*, **76**, 8517-8533.

PAPAZACHOS, B.C., A.A. KIRATZI and E.E. PAPADIMITRIOU (1991): Regional focal mechanisms for earthquakes in the Aegean area, *Pure Appl. Geophys.*, **136**, 405-420.

PAPAZACHOS, B.C., A.A. KIRATZI and E.E. PAPADIMITRIOU (1992): Orientation and type of faulting in the Aegean and the surrounding area, *Bull. Geol. Soc. Greece* (in press).

TAYMAZ T., J.A. JACKSON and D. MC KENZIE (1991): Active tectonics of the North an Central Aegean Sea, *Geophys. J. Int.*, **106**, 433-490.

(received March 22, 1994;
accepted September 10, 1994)